AD-A188 158 HIGH TEMPERATURE OXIDATION STUDIES ON ALLOYS CONTAINING 1/1
DISPERSED PHASE P.. (U) PENNSYLVANIA STATE UNIV
UNIVERSITY PARK B MUNN ET AL. SEP 87 AFOSR-TR-87-1688
UNCLASSIFIED AFOSR-85-0298 F/G 11/6.1 NL

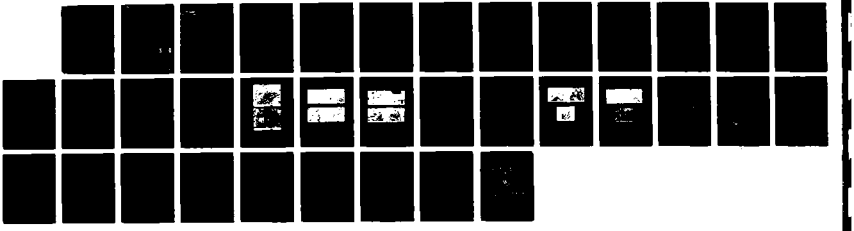

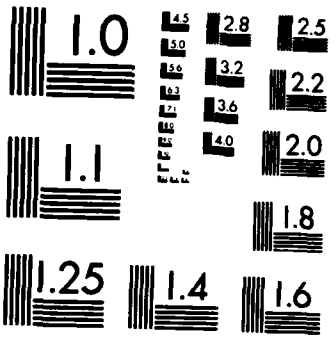

(2)

AFOSR-TR- 87-1688

Grant No.AFOSR-85-0298

Second Annual Report

to

Air Force Office of Scientific Research
Bolling, AFB, DC 20332

HIGH TEMPERATURE OXIDATION STUDIES ON ALLOYS CONTAINING DISPERSED PHASE PARTICLES AND CLARIFICATION OF THE MECHANISM OF GROWTH OF SiO_2

Submitted to: Maj. Joseph W. Hager

Submitted by: B. Munn, S. W. Park and G. Simkovich

September 1987

SECURITY CLASSIFICATION OF THIS PAGE

AI88 158

REPORT DOCUMENTATION PAGE

1a. REPORT SECURITY CLASSIFICATION: UNCLASSIFIED	1b. RESTRICTIVE MARKINGS
2a. SECURITY CLASSIFICATION AUTHORITY: UNCLASSIFIED	3. DISTRIBUTION/AVAILABILITY OF REPORT: Approved for public release, distribution unlimited
2b. DECLASSIFICATION/DOWNGRADING SCHEDULE	
4. PERFORMING ORGANIZATION REPORT NUMBER(S)	5. MONITORING ORGANIZATION REPORT NUMBER(S): AFOSR-TR- 1688
6a. NAME OF PERFORMING ORGANIZATION: Pennsylvania State University	6b. OFFICE SYMBOL (If applicable):
7a. NAME OF MONITORING ORGANIZATION: AFOSR	
6c. ADDRESS (City, State and ZIP Code): University Park PA	7b. ADDRESS (City, State and ZIP Code): Bldg 410 Bolling AFB, DC 20332-6448
8a. NAME OF FUNDING/SPONSORING ORGANIZATION: SAME AS 7a	8b. OFFICE SYMBOL (If applicable): NE
9. PROCUREMENT INSTRUMENT IDENTIFICATION NUMBER: AFOSR-85-0298	
8c. ADDRESS (City, State and ZIP Code): SAME AS 7b	10. SOURCE OF FUNDING NOS.

PROGRAM ELEMENT NO.	PROJECT NO.	TASK NO.	WORK UNIT NO.
61102F	2306	A2	

11. TITLE (Include Security Classification): High Temperature Oxidation Studies on Alloys Containing Dispersed Phase Particles and Clarification of the Mechanism of Growth of SiO_2

12. PERSONAL AUTHOR(S): Dr Simkovich

13a. TYPE OF REPORT	13b. TIME COVERED	14. DATE OF REPORT (Yr., Mo., Day)	15. PAGE COUNT
Annual Report	FROM 15Aug86 TO 14Aug87	Sep 1987	

16. SUPPLEMENTARY NOTATION

17. COSATI CODES			18. SUBJECT TERMS (Continue on reverse if necessary and identify by block number)
FIELD	GROUP	SUB. GR.	

19. ABSTRACT (Continue on reverse if necessary and identify by block number)

In the present investigation, the effects of dispersed SiO_2 particles on the high temperature oxidation behavior of Ni-Cr and Fe-Cr alloys were studied. This study differs from previous investigations in that larger volume percents of SiO_2 (5-40 vol%) were incorporated into the alloys.

Kinetic studies were done using an automatic recording semi-micro balance under the desired conditons (1 atm O_2 and 1273, 1373K). Surface topographies of oxidized specimens were also prepared and examined optically and by scanning electron microscopy. Standard x-ray diffraction techniques were employed to identify the phases present in the scale. Based upon extensive results obtained for the Ni-Cr-SiO_2 alloy a model for oxide formation in this systme is proposed. The results obtained for the Fe based system will also be presented in this report.

20. DISTRIBUTION/AVAILABILITY OF ABSTRACT	21. ABSTRACT SECURITY CLASSIFICATION
UNCLASSIFIED/UNLIMITED ☐ SAME AS RPT. ☐ DTIC USERS ☐	UNCLASSIFIED

22a. NAME OF RESPONSIBLE INDIVIDUAL	22b. TELEPHONE NUMBER (Include Area Code)	22c. OFFICE SYMBOL
MAJ HAGER	202 767-4933	NE

DD FORM 1473, 83 APR — EDITION OF 1 JAN 73 IS OBSOLETE.

SECURITY CLASSIFICATION OF THIS PAGE

INTRODUCTION

In binary Ni-Cr, Fe-Cr, and Co-Cr alloys Cr is an alloying element used to increase the oxidation resistance of these alloys. This alloying addition allows for the formation of a protective Cr_2O_3 layer, but in order for this layer to form completely, the Cr content in the alloy must exceed a critical value. This critical Cr content is a function of the base metal, and for the metals of interest is usually greater than 18 wt% Cr.

It has been established that the presence of a finely distributed oxide or nitride phase markedly affects the oxidation behavior of these binary alloys at high temperatures. The oxidation rates are decreased dramatically, and scale adhesion to the underlying alloy is improved in some cases. However, investigations in this area have been limited to 1-2 vol% additions of a dispersed phase.

In the present investigation, the effects of dispersed SiO_2 particles on the high temperature oxidation behavior of Ni-Cr and Fe-Cr alloys were studied. This study differs from previous investigations in that larger volume percents of SiO_2 (5-40 vol%) were incorporated into the alloys.

Kinetic studies were done using an automatic recording semi-micro balance under the desired conditions (1 atm O_2 and 1273, 1373K). Surface topographies of oxidized specimens were studied by scanning electron microscopy. Transverse sections of representative specimens were also prepared and examined optically and by scanning electron microscopy. Standard x-ray diffraction techniques were employed to identify the phases present in the scale.

Based upon extensive results obtained for the Ni-Cr-SiO_2 alloys, a model for oxide formation in this system is proposed. The results obtained for the Fe based system will also be presented in this report.

Ni-Cr-SiO_2 System

Results from previous investigations demonstrated that the addition of SiO_2 particles into Ni-Cr alloys increase the oxidation resistance by many orders of magnitude as shown in Figures 1-4. The increase in oxidation resistance is due to the formation of a protective Cr_2O_3 scale. This scale was found to exist in alloys containing Cr contents as low as 6 wt%. In most commercial Ni-Cr alloys 18 wt% Cr is necessary to form a protective Cr_2O_3 scale.

To clarify the mechanism of scale formation on Ni-Cr-SiO_2 alloys, time dependent oxidation tests were preformed on selected Ni-Cr alloys with and without SiO_2 particles. Table I shows compositions of the alloys used in this study. Each alloy was oxidized for a predetermined time under the desired conditions (1 atm O_2, 1273K). The oxide scale that formed was then examined by scanning electron microscopy and x-ray diffraction analysis to determine the oxides present.

Figures 5-7 show oxide surface topographies formed on Ni-6Cr-SiO_2 alloys as a function of volume percent SiO_2 particles after oxidizing for 4 min - 3 hrs. at 1273K.

The entire surface of the binary Ni-6Cr alloy was covered with a uniform layer of NiO. As time progresses, the NiO scale grows continuously outward. However, a non-uniform NiO scale developed on the oxide surface of Ni-6Cr-SiO_2 alloys. This relatively thin scale formed adjacent to the SiO_2 particles on the surface, with Cr_2O_3 scale formation occurring at the interface between the NiO and SiO_2 particles as shown in Figure 5.

Figure 6 shows the surface topographies of various Ni-6Cr alloys with and without additions of SiO_2. Upon addition of 10 vol% SiO_2, an increase in the grain size of NiO was observed. Also, SiO_2 particles begin to appear at the surface of this alloy. The surface topographies of Ni-6Cr alloys containing 20

and 40 vol% SiO_2 show a further enlargement in the NiO grain size, and a larger number of SiO_2 particles visible on the surface. Consequently, the inward diffusion of oxygen ions or atoms is favored, and the protective Cr_2O_3 scale can easily form underneath the initially formed NiO scale.

The preferential formation of Cr_2O_3 adjacent to SiO_2 particles seems to be the result of an increase in Cr diffusion along the grain boundaries. The addition of SiO_2 reduces the grain size of the base material as shown in Figure 8. The reduction in grain size results in an increased grain boundary area. Since the SiO_2 appears to be predominant at the grain boundaries, an increase in grain boundary area would lead to a greater number of Cr atoms reaching the surface at or near an SiO_2 particle. A schematic representation of the oxide formation and the involved ion or metal transport during an initial oxidation period on Ni-6Cr-SiO_2 alloys is shown in Figure 9.

Figures 10 and 11 show the oxide surface topographies of Ni-9Cr-20 vol% SiO_2, Ni-12Cr-10 vol% SiO_2, and Ni-15Cr-20 vol% SiO_2 alloys after oxidizing for 10 min and 2 hrs at 1273K in 1 atm O_2. The oxide scale formed on these alloys are quite different from those formed on Ni-6Cr-SiO_2 alloys. After oxidizing for 10 min, a Cr_2O_3 scale with minor amounts of NiO formed on these alloys. It seems that the increased Cr content may enhance both Cr grain boundary diffusion as well as bulk diffusion. As a result of preferential Cr diffusion through grain boundaries as well as along the SiO_2/alloy interfacial boundaries, a relatively thick Cr_2O_3 scale formed adjacent to the incorporated SiO_2 particles.

In this study, several models are proposed to explain the mechanism of oxide formation of Ni-Cr-SiO_2 alloys containing intermediate Cr contents (6-15 wt%) including the binary Ni-6Cr alloy.

Figure 12 is a schematic representation of the oxide scale formation on the Ni-6Cr alloy as proposed by Wood (1). Since the Cr content in the binary Ni-6Cr

alloy is not sufficient to yield a complete Cr_2O_3 layer, the initially formed Cr_2O_3 is easily overgrown by NiO during early stages of oxidation.

The presence of SiO_2 particles in the Ni-6Cr alloy markedly changes the mechanism of oxide formation. The increased grain boundary and interfacial boundary area enhances the transport of Cr in the metal phase. The accelerated Cr transport along such boundaries may be sufficient to yield a protective Cr_2O_3 layer during an early stage of oxidation as shown in Figure 13. As the volume percent of SiO_2 in the Ni-6Cr alloy increased, the grain size of the alloy and spacing between particles was reduced as shown in Figure 9. Therefore, a protective Cr_2O_3 layer can be developed at an earlier stage of oxidation due to an increase in short circuit paths, as well as a reduction in spacing between initially formed Cr_2O_3 particles. Increasing additions of Cr result in a more rapid formation of the Cr_2O_3 scale due to the enhancement of Cr transport through short circuit paths as well as the alloy matrix.

The parabolic oxidation rate constants of Ni-Cr-SiO_2 alloys are compared with those of pure Cr from previous experimental work (2,3). The calculated oxidation rate was determined from values of diffusion constants of Cr ions in Cr_2O_3 as reported by Kofstard and Lillerod (4). Figure 14 shows that the Kp values of Ni-Cr-SiO_2 alloys are orders of magnitude smaller than those for pure Cr at various oxidation temperatures. This is believed to be due to the presence of SiO_2 particles in the Cr_2O_3 scale, which may alter the ionic transport mechanisms in the scale.

Recently, Atkinson and Taylor (5) have found that the most likely process which controls the Cr_2O_3 film growth is Cr ion diffusion along grain boundaries but not via dislocations. Chromium diffusion in polycrystalline Cr_2O_3 was found to be several orders of magnitude faster than that in single crystal Cr_2O_3 (6,7). It is obvious that the transport rate of Cr ions along grain boundaries

is increased. Therefore, the oxidation rate of alloys containing stable oxide particles is expected to be increased compared to the pure Cr. However, the oxidation rate of these alloys and Ni-Cr-SiO_2 alloys in this study have been found to be lower than that of pure Cr or Ni-20 Cr alloy.

For alloys containing stable oxide particles, fast Cr diffusion along grain boundaries in Cr_2O_3 is impeded due to the presence of dispersed oxide particles in the oxide scale. Hence the growth rate of Cr_2O_3 is reduced.

In the present investigation, the change in the volume percent of SiO_2 particles in Ni-Cr alloys has a minor effect on the oxidation rate after formation of a continuous Cr_2O_3/SiO_2 oxide scale. This indicates that after a certain concentration of particles is present, further addition of SiO_2 will not aid in the blocking of Cr diffusion through the scale. However, according to the suggested model for oxide formation on Ni-Cr-SiO_2 alloys, the grain size of Cr_2O_3 formed was reduced as the volume percent of SiO_2 was increased. Consequently, the grain boundary area available for rapid Cr diffusion increased. However, more SiO_2 particles are available for blocking Cr diffusion through the grain boundaries of the Cr_2O_3 scale. Although there is no means to calculate the minimum amount of oxide dispersions necessary to block Cr diffusion along grain boundaries, it would appear from this study that relatively small amounts of oxide particles (on the order of 5 vol%) in Cr_2O_3 effectively block rapid Cr diffusion along grain boundaries. This indicates that the amount of oxide particles necessary to impede grain boundary diffusion of Cr ions is not significantly different from that presently utilized in commercial alloys. The addition of larger volume percents of a dispersed phase increases the oxidation resistance, but the resistance increase beyond about 10 vol% is not appreciable.

Fe-Cr-SiO_2 Alloy System

Figures 15 and 16 show the kinetic behavior of pure Fe alloys containing various amounts of SiO_2 particles at 1273 and 1373 K. The experiments were conducted in 1 atm O_2 for approximately 50 hrs. The incorporation of 5 vol% of dispersed SiO_2 particles increased the oxidation resistance of the alloy in both cases. Upon increasing the SiO_2 content, further increase in resistance was observed at 1273 K. However, no general trend seems to be evident when additions of greater than 5 vol% were incorporated into the Fe alloy.

Figure 17 and 18 show the kinetic behavior of the binary Fe-9Cr alloy at 1273 and 1373 K. In both cases a significant weight gain occurred, indicating a low oxidation resistance under these conditions.

Figures 19 and 20 show the kinetic behavior of Fe-9Cr alloys containing SiO_2 particles in concentrations between 5-20 vol%. At a concentration of 5 vol% SiO_2, a considerable increase in oxidation resistance was achieved. During an initial period of oxidation, the Fe-9Cr alloy with 5 vol% SiO_2 displayed similar oxidation kinetics to that of the binary Fe-9Cr alloy. However, after a period of time, the oxidation rate was markedly reduced. Further additions of SiO_2 showed similar kinetic behavior to that of the Fe-9Cr-5 vol% SiO_2 alloy. The increase in oxidation resistance in these alloys is apparently due to the formation of a protective oxide scale.

Figure 21 depicts the calculated parabolic rate constants for Fe-9Cr-SiO_2 alloys versus volume percent SiO_2. Compared to that of the binary Fe-9Cr alloy, the rate constant for Fe-9Cr-5 vol% SiO_2 is considerably less. This dramatic decrease in the rate constant is indicative of the formation of a protective oxide scale. Further increases in the SiO_2 content decrease the rate constant, but not to a significant degree when compared to the initial decrease observed upon addition of 5 vol% SiO_2.

Figure 22 shows the kinetic behavior of five Fe-Cr alloys with a constant SiO_2 content (20 vol%) at 1273K. At 6 wt% Cr, there is no evidence of the formation of a complete, protective scale during the duration of the experiment. However, at 9 wt% Cr, a complete protective scale has apparently formed. Therefore, the critical Cr content necessary to form a protective scale falls in the region between 6-9 wt% Cr. Hence, the addition of 20 wt% SiO_2 to binary Fe-Cr alloys reduces the Cr content necessary to form a protective layer from approximately 18 wt% to 6-9 wt%.

The presence of SiO_2 in binary Fe-9Cr alloys dramatically reduced the oxidation rate by the formation of a protective oxide scale. The scale that formed was complex, but is is believed that the formation of a protective Cr_2O_3 scale is primarily responsible for the considerable reduction in oxidation rates. Further evidence of a protective Cr_2O_3 layer can be seen in the considerable drop that occurs in the parabolic rate constants in Figure 20. This decrease can only be attributed to the formation of a protective Cr_2O_3 scale. Also, x-ray diffraction studies of the scale revealed the presence of Cr_2O_3 in the oxide scale.

SiO_2 Growth Studies

A number of tests, all unsuccessful, were made in an attempt to elucidate on the mechanism of SiO_2 growth. Basically, all of these tests consisted of placing, under pressure, an inert electronic oxide conductor on the surface of silicon and then oxidizing in air or oxygen to determine whether the electronic short circuit provided by the non-reacting oxide accelerated the growth of the SiO_2 scale.

Two observations were made. These were: (1) the difference between the scale thickness at various points across the sample was not sufficient to alloy any conclusions to be drawn; and, (2) there was much difficulty in ascertaining

the scale thickness adjacent to the "inert" oxide phase.

Future attempts will be made utilizing Cr_2O_3 particles pressed on one sample of silicon and oxidizing at a given temperature and oxygen pressure. Under identical conditions a silicon sample, from the same batch of silicon as utilized in the previous run, will be oxidized. A comparison of the scales will then be made.

REFERENCES

1. O. Kubachewski and B. E. Hopkins, Oxidation of Metals and Alloys, Butterworth London (1962).

2. L. Cadiou and J. Paidassi, Mem. Sci. Rev. Metall., 66, 217 (1969).

3. K. P. Lillerud and P. Koftsad, J. Electrochem. Soc., 127, 2397 (1980).

4. P. Kofstad and K. P. Lillerud, ibid, 2411 (1980).

5. H. Nagai, F. Koshi-ishi, S. IshiKawa, and K. Shoji, Trans. Japn. Inst. Metal., 24, 839 (1983).

6. C. S. Giggins and F. S. Pettit, Met. Trans., 2, 1071 (1971).

7. J. Stringer, B. A. Wilcox, and R. I. Jaffec, Oxid. Met., 5, 11 (1972).

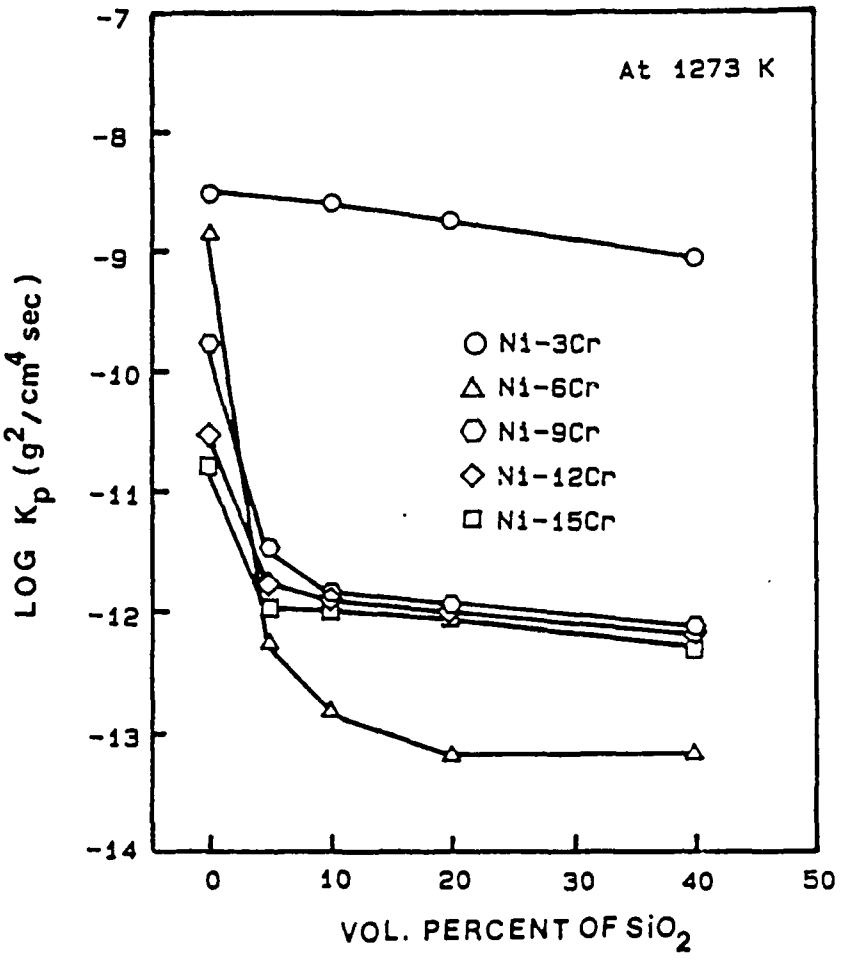

Figure 1. Parabolic oxidation rates of Ni-Cr-SiO_2 alloys as a function of the volume percent of SiO_2 dispersions at 1273K.

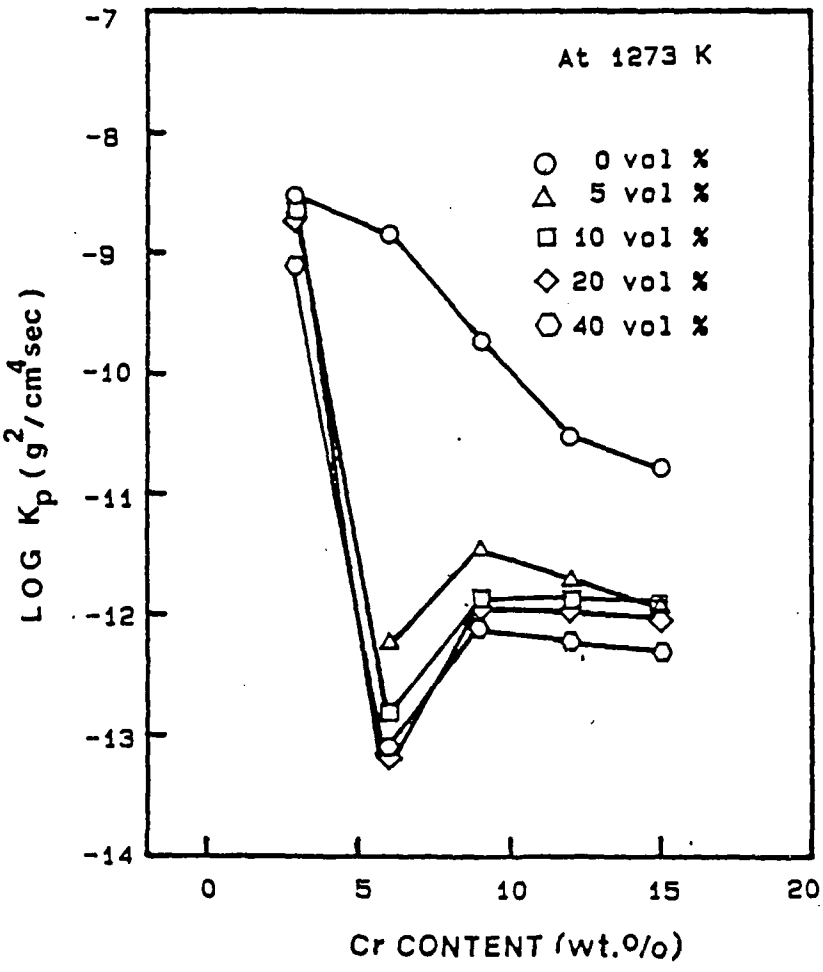

Figure 2. Parabolic oxidation rates of Ni-Cr-SiO_2 alloys as a function of Cr contents at 1273K.

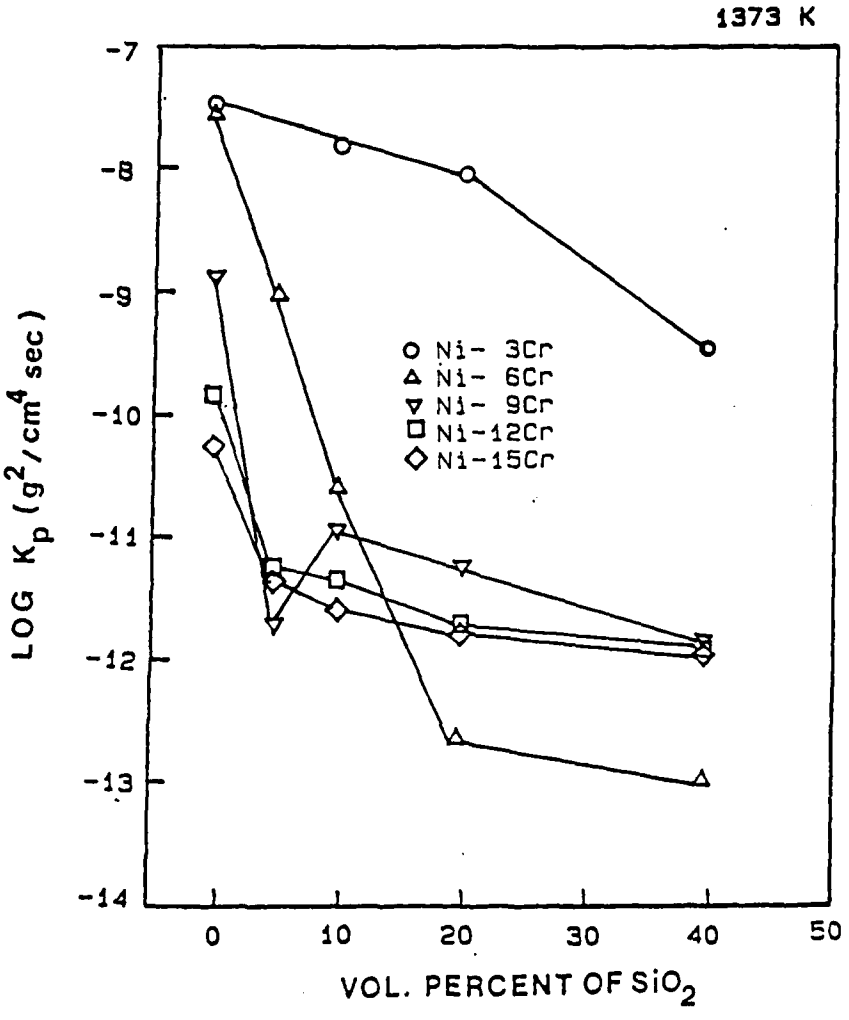

Figure 3. Parabolic oxidation rates of Ni-Cr-SiO_2 alloys as a function of the volume percent of SiO_2 dispersions at 1373 K.

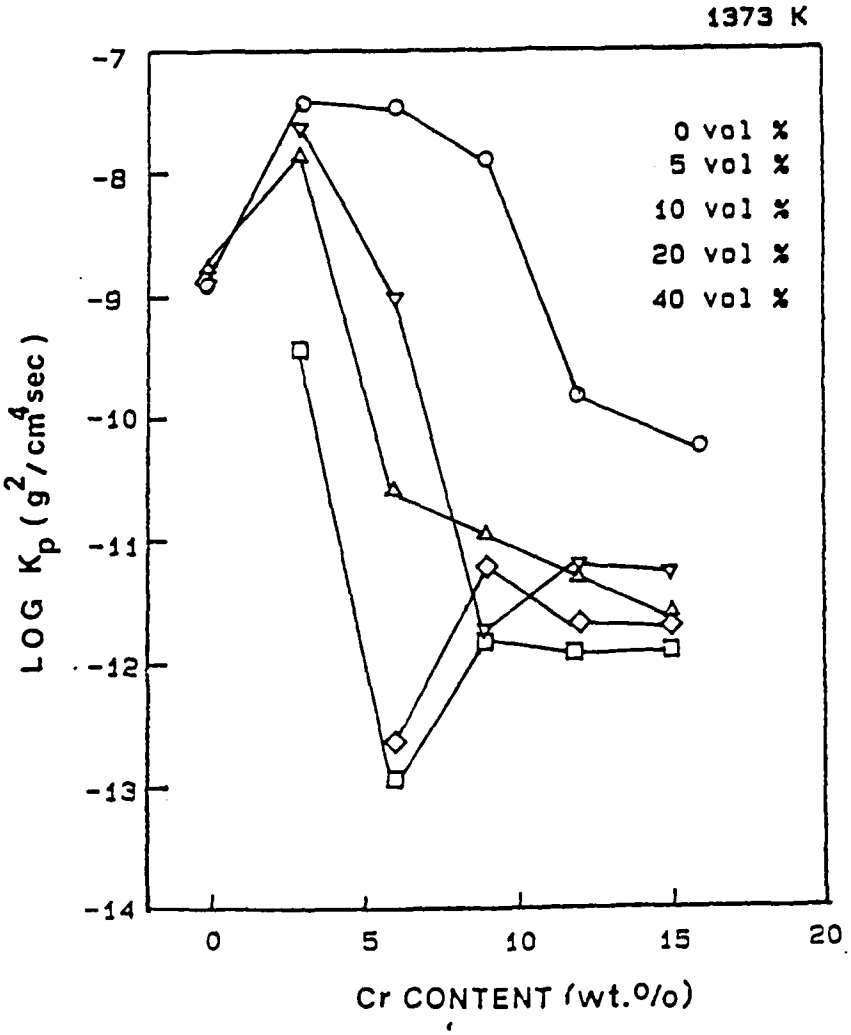

Figure 4. Parabolic oxidation rates of Ni-Cr-SiO_2 alloys as a function of Cr contents at 1373 K.

Table 1

The characteristics of the powders.

Materials	Purity	Particle Size	Remarks
Ni	99.5%	2.5 μm - 3 μm	
Cr	99.5%	2 μm	
Si	99%	2 μm	
SiO_2	99.8%	30 - 300 Å	amorphous Cal-O-Sil M-5
TiO_2	99.6%	less than 1 μm	
Al_2O_3	99.6%	less than 1 μm	
ThO_2	99%	10 μm	

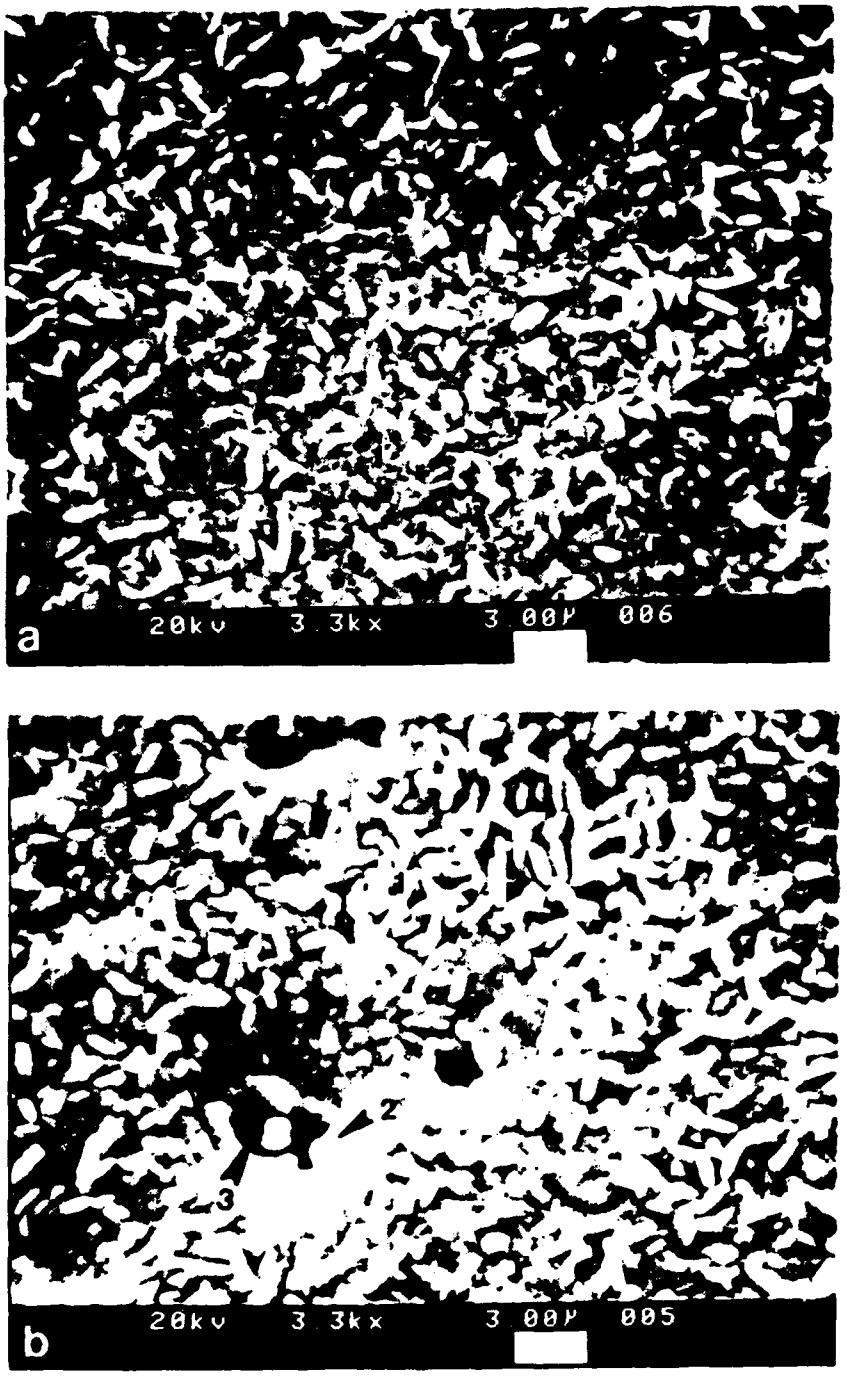

Figure 5. Surface topographies of (a) binary Ni6Cr alloy and (b) Ni-6Cr-10 vol% SiO_2 alloy after oxidizing for 4 min. at 1273 K in 1 atm. O_2. 1: NiO 2: Cr_2O_3 3: SiO_2

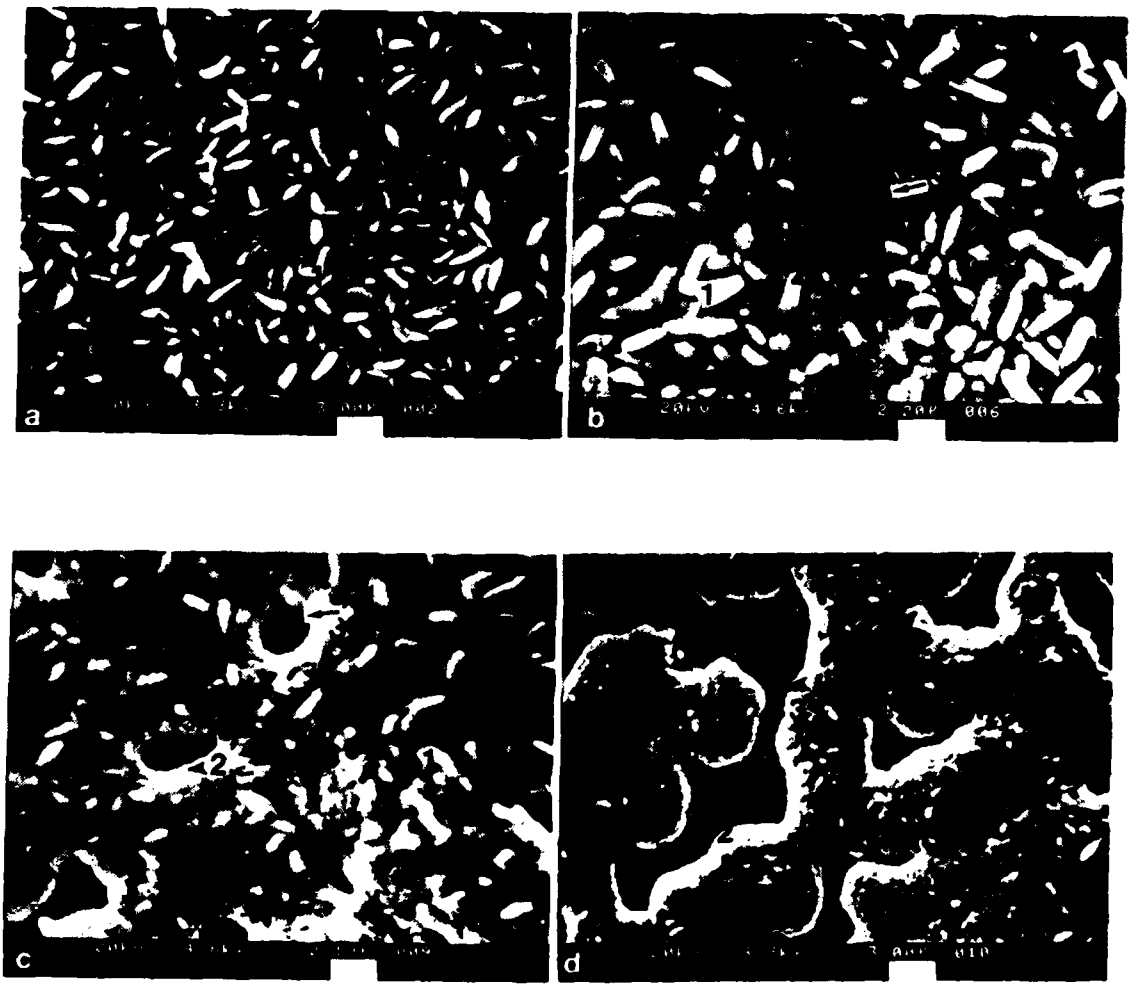

Figure 6. Surface topographies of (a) binary Ni-6Cr alloy and (b) Ni-6Cr-10 vol% SiO_2 alloy, (c) Ni-6Cr-20 vol% SiO_2 alloy, and (d) Ni-6Cr-40 vol% SiO_2 alloy after oxidizing for 10 min. at 1273 K. 1: NiO 2: Cr_2O_3 3: SiO_2

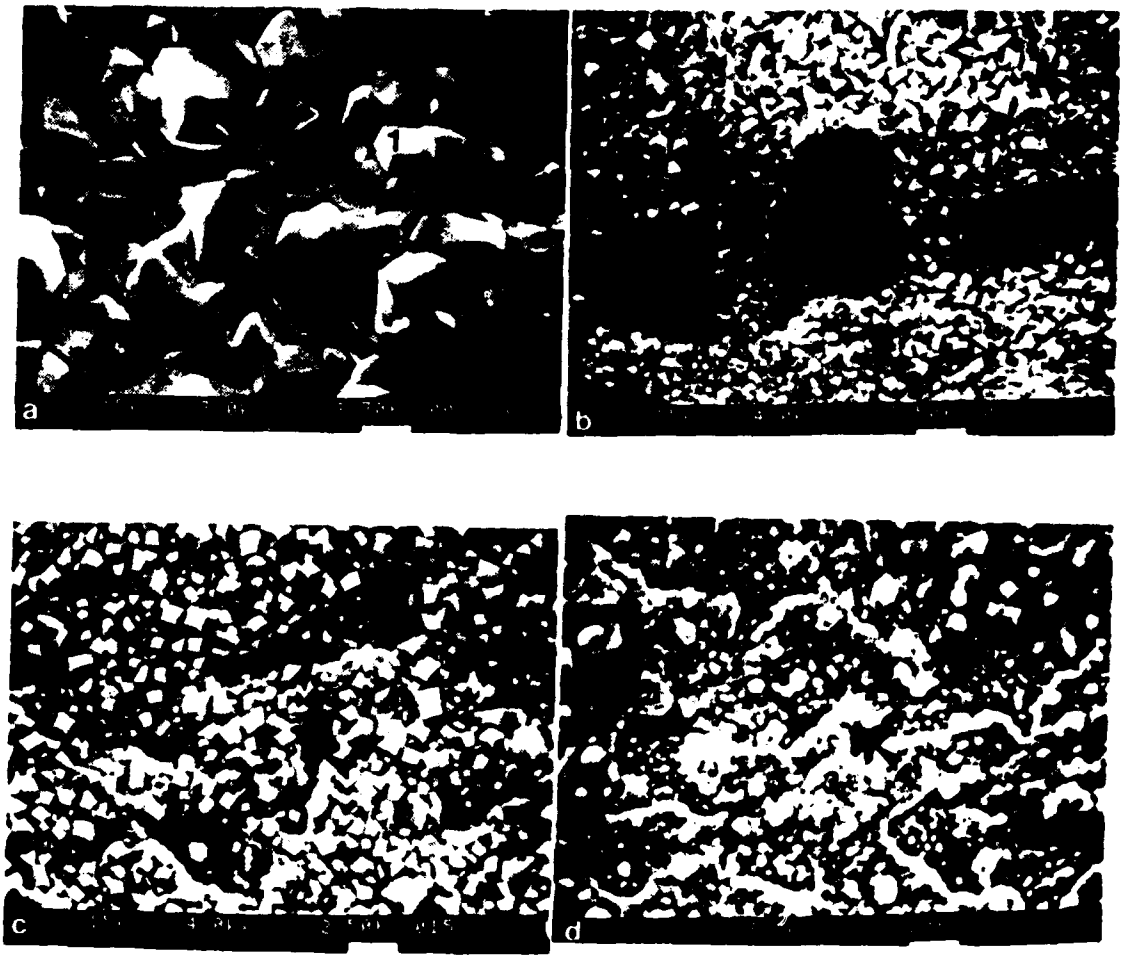

Figure 7. Surface topographies of (a) binary Ni-6Cr alloy, (b) Ni-6Cr-10 vol% SiO_2 alloy, (c) Ni-6Cr-20 vol% SiO_2 alloy, and (d) Ni-6Cr-40 vol% SiO_2 alloy after oxidizing for 3 hours at 1273 K. 1: NiO 2: Cr_2O_3 3: $NiO/NiCr_2O_4$ 4: SiO_2

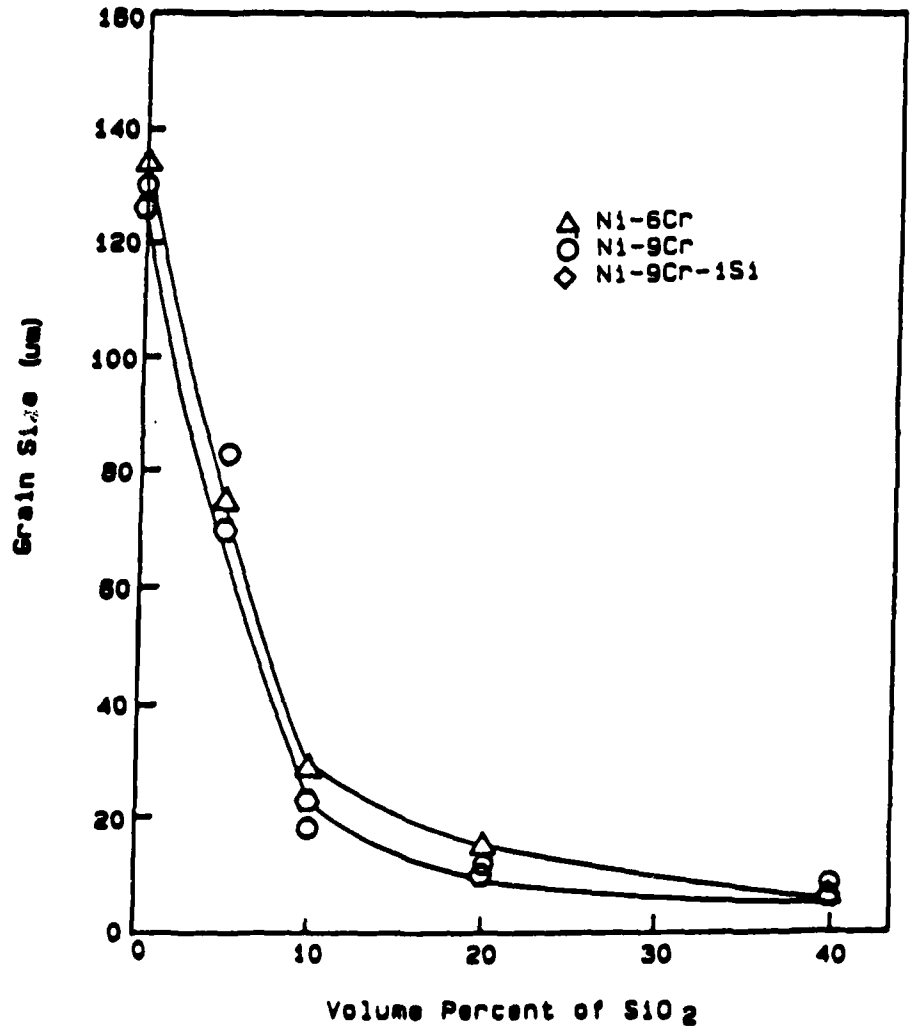

Figure 8. The average grain size of the Ni-6Cr-SiO_2, Ni-9Cr-SiO_2, and Ni-9Cr-1Si-SiO_2 alloys as a function of the volume percent of SiO_2 dispersions in the alloy.

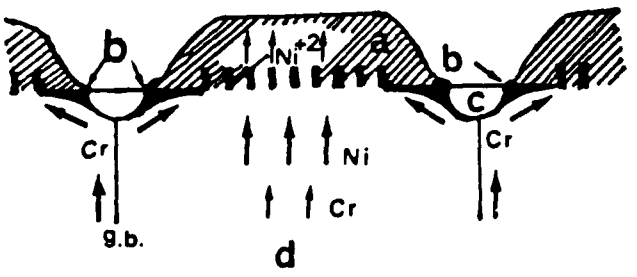

Figure 9. Schematic representation of the oxide formation and the involved ion transport during an initial oxidation period on Ni-6Cr-SiO_2 alloys. a: NiO b: Cr_2O_3 c: SiO_2 d: alloy.

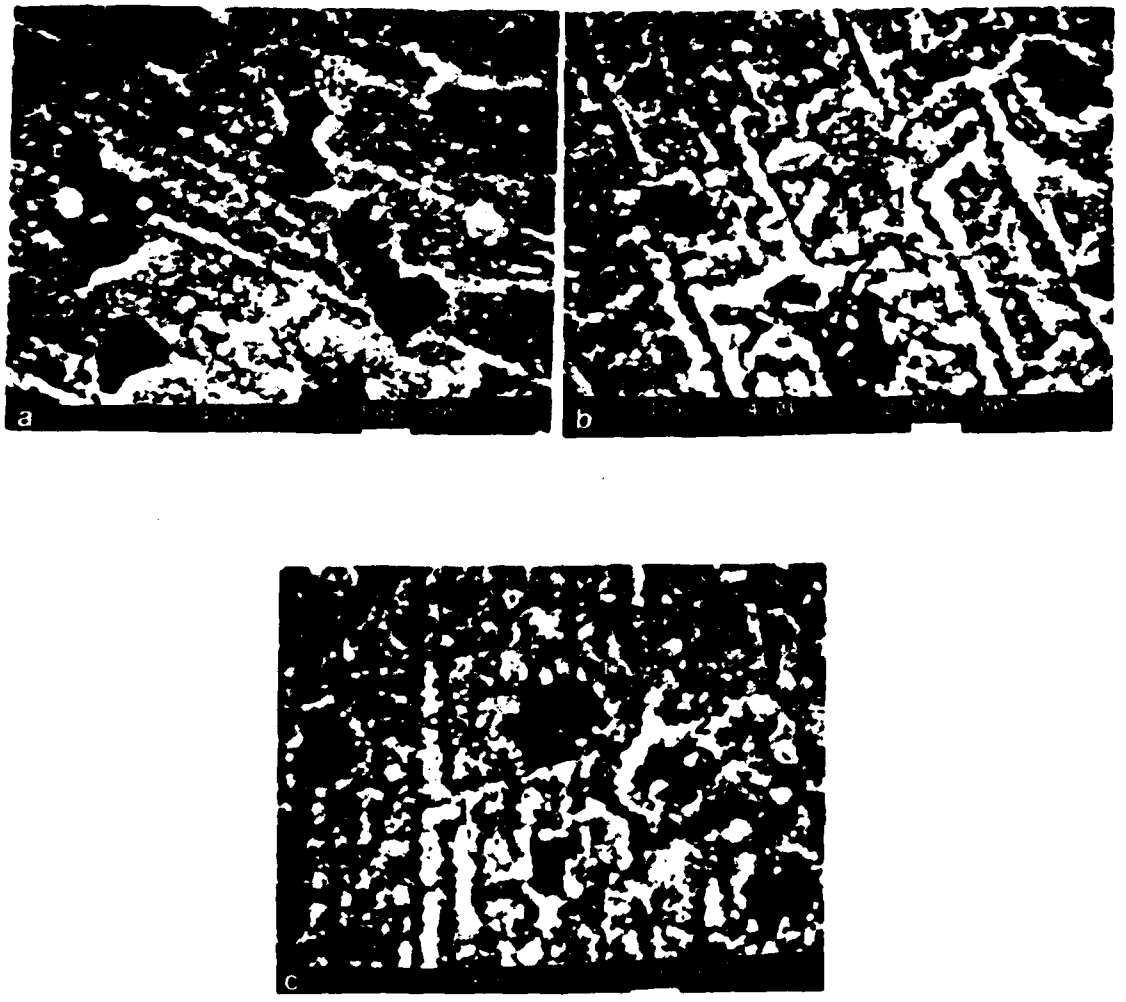

Figure 10. Surface topographies of (a) the Ni-9Cr-20 vol% SiO_2 alloy, (b) the Ni-12Cr-10 vol% SiO_2 alloy, and (c) the Ni-15Cr-20 vol% SiO_2 alloy after oxidizing for 10 min. at 1273 K. 1: Cr_2O_3 with small amount of NiO 2: SiO_2

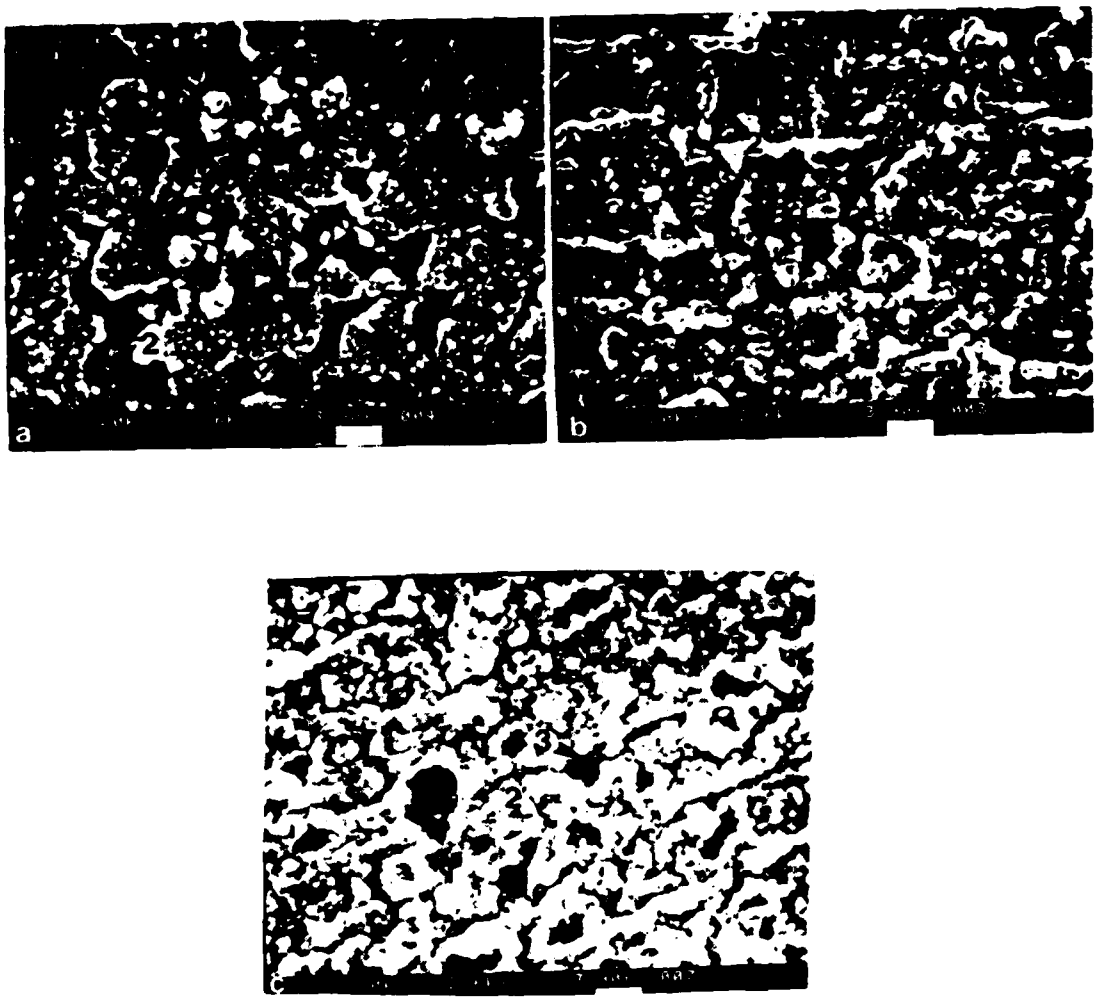

Figure 11. Surface topographies of (a) the Ni-9Cr-20 vol% SiO_2 alloy, (b) the Ni-12Cr-10 vol% SiO_2 alloy, and (c) the Ni-15Cr-20 vol% SiO_2 alloy after oxidizing for 2 hours at 1273 K. 1: $NiO/NiCr_2O_4$ 2: Cr_2O_3 3: SiO_2

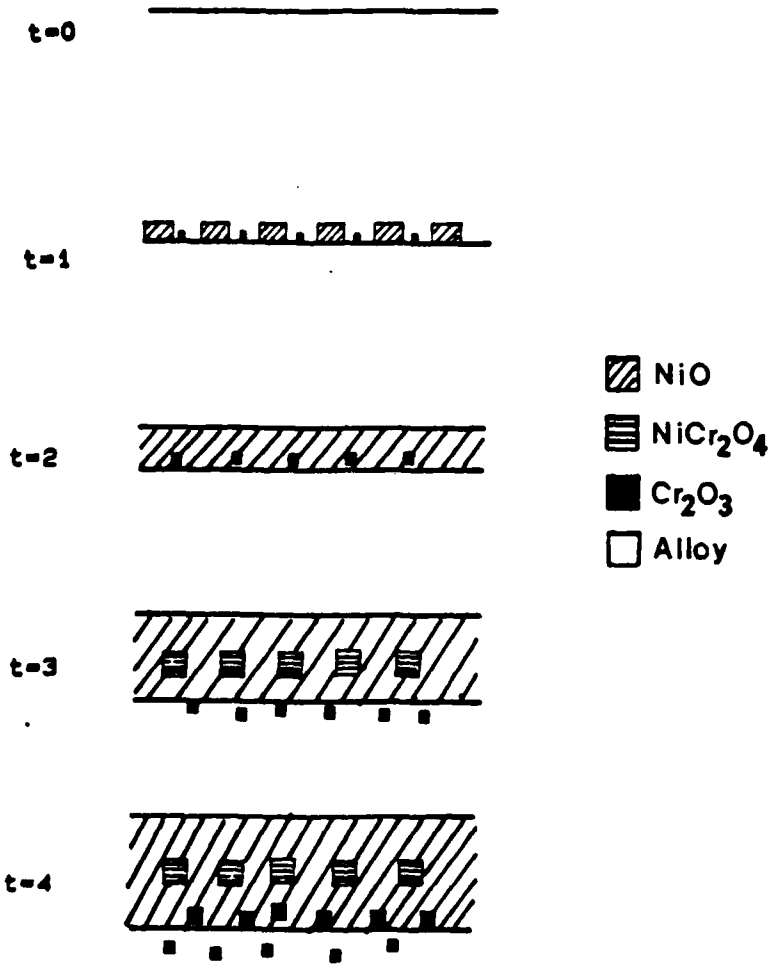

Figure 12. Schematic representation of the oxide formation on binary Ni-6Cr alloy.

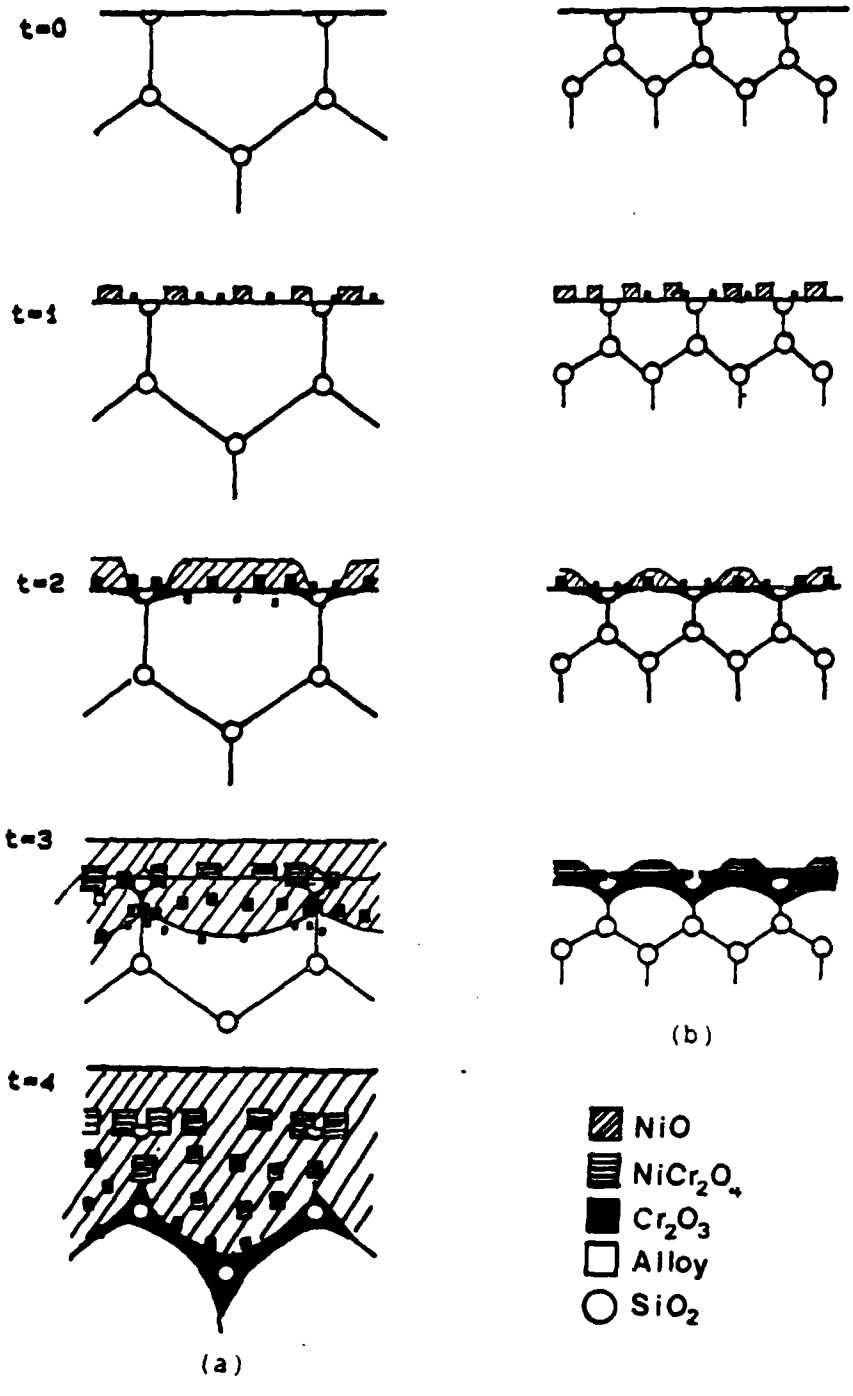

Figure 13. Schematic representation of the oxide formation on the Ni-6Cr-SiO_2 alloys. (a) low volume percent of SiO_2 (b) high volume percent of SiO_2.

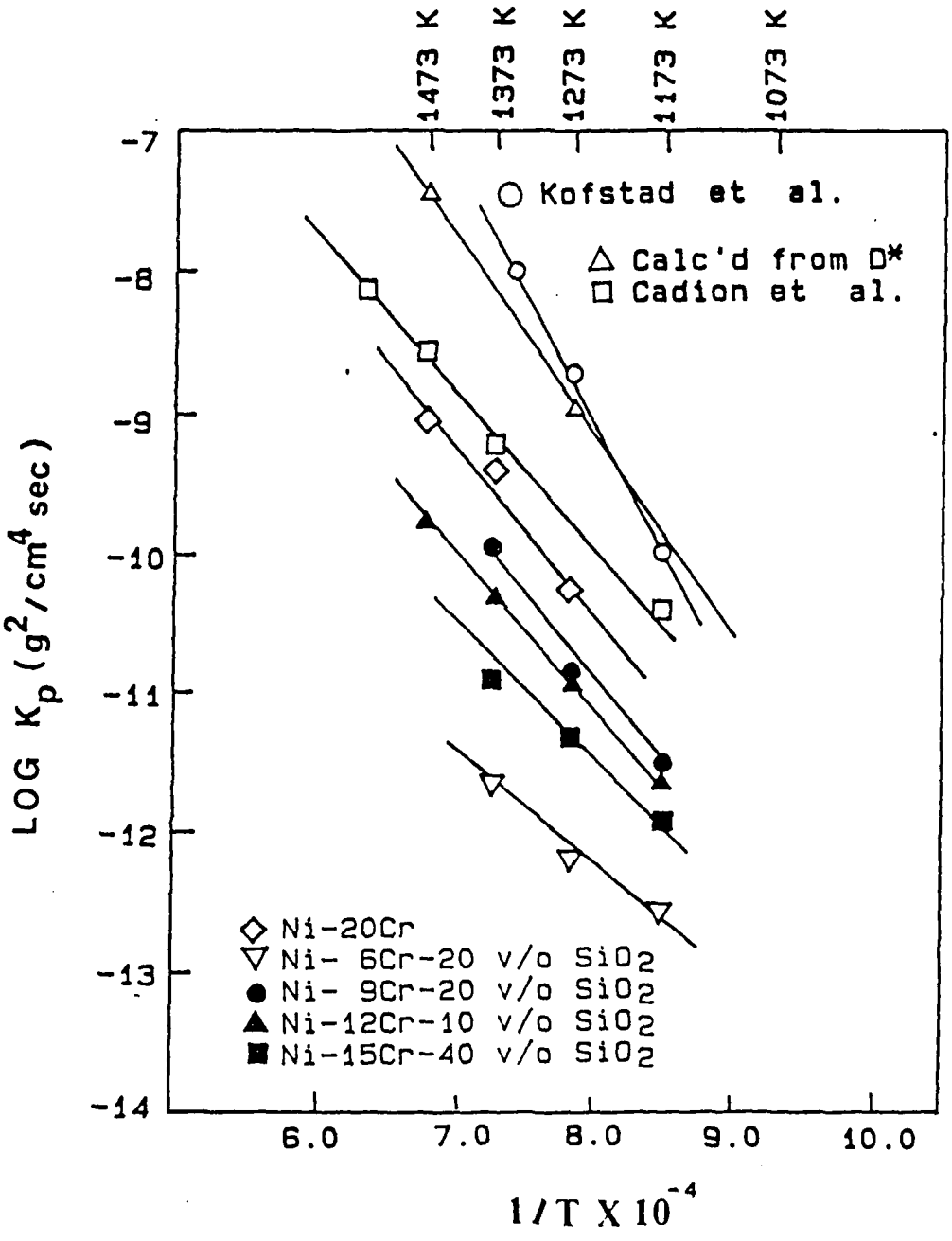

Figure 14. Parabolic oxidation rates of binary Ni-20Cr, Ni-6Cr-20 vol% SiO_2, Ni-9Cr-20 vol% SiO_2, Ni-12Cr-10 vol% SiO_2, and Ni-15Cr-40 vol% SiO_2 alloys and pure Cr from previous investigations. Kofstad and Lillerud (4) and calculated from D_{Cr*} (3) and Cadiou et al. (2).

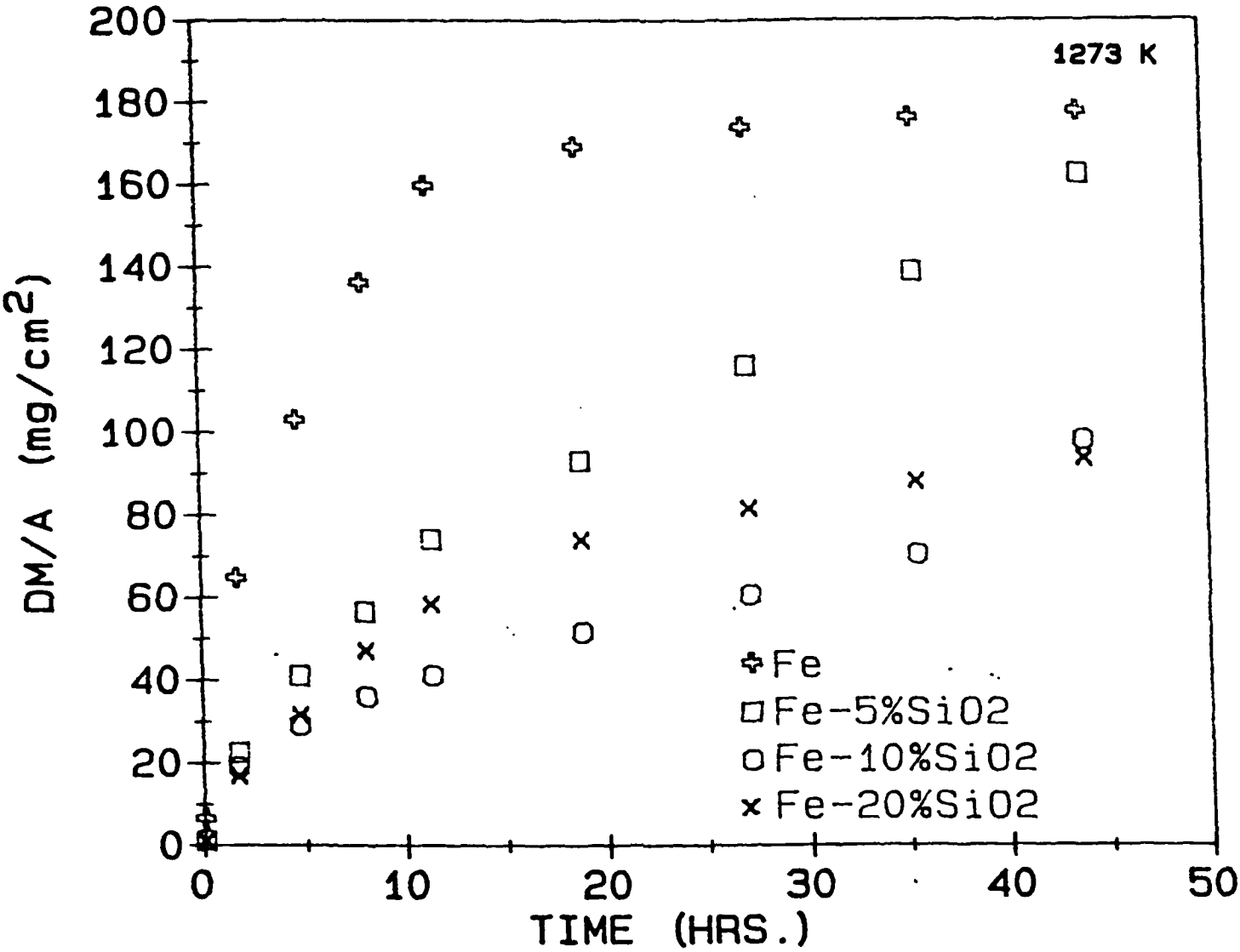

Figure 15. Isothermal oxidation curves for Fe-SiO_2 alloys at 1273 K.

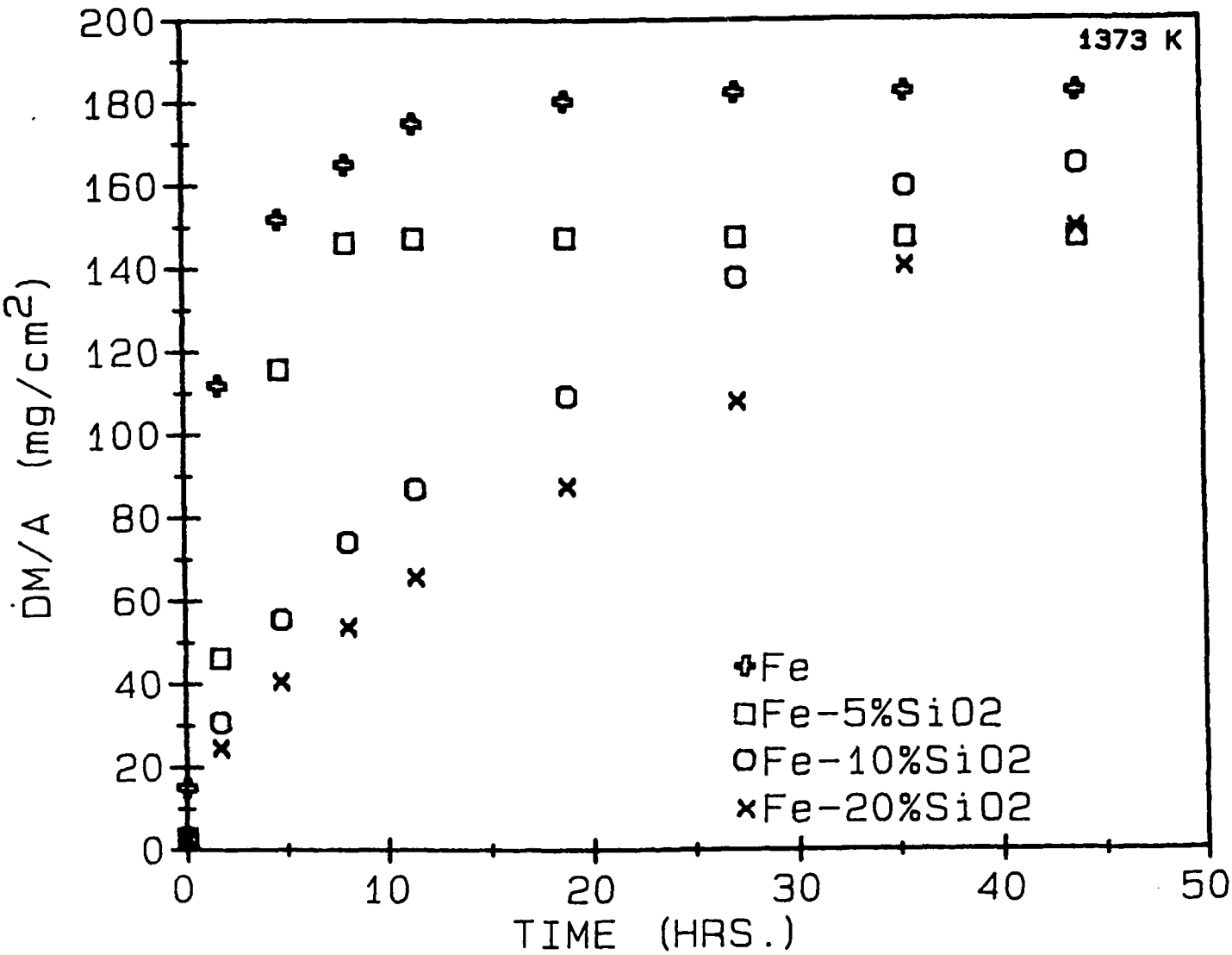

Figure 16. Isothermal oxidation curves for Fe-SiO_2 alloys at 1373 K.

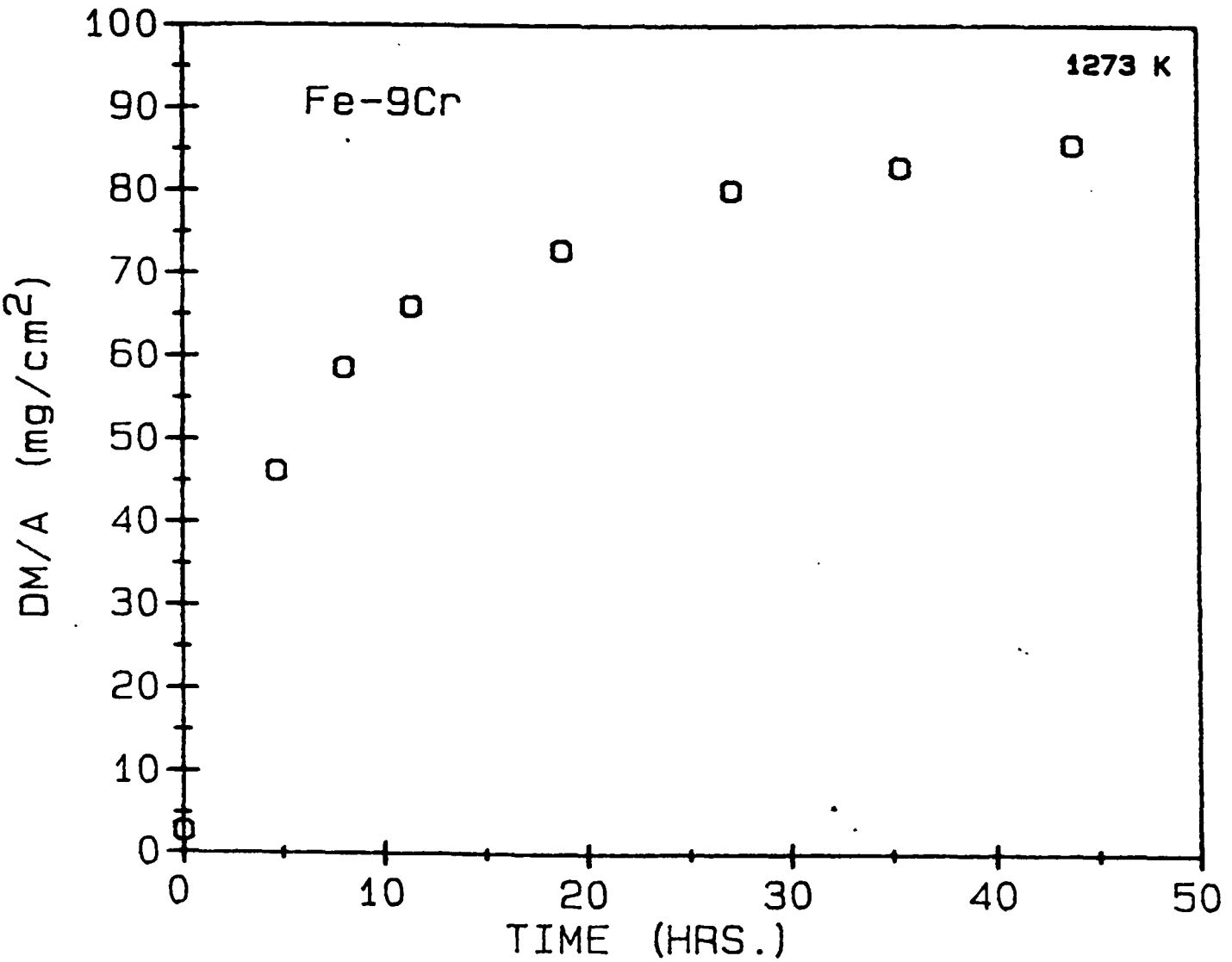

Figure 17. Isothermal oxidation curve for binary Fe-9Cr alloy at 1273 K.

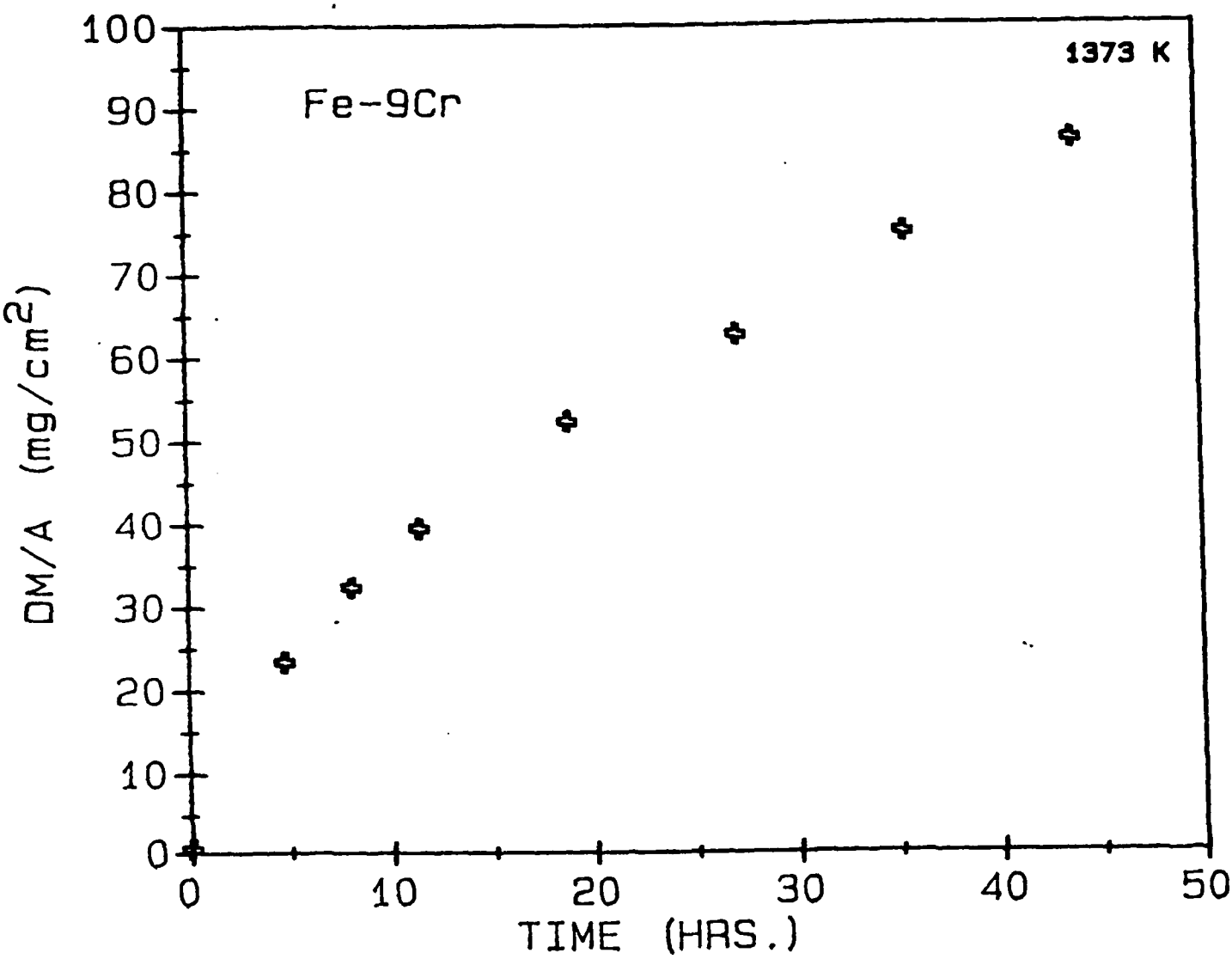

Figure 18. Isothermal oxidation curve for binary Fe-9Cr alloy at 1373 K.

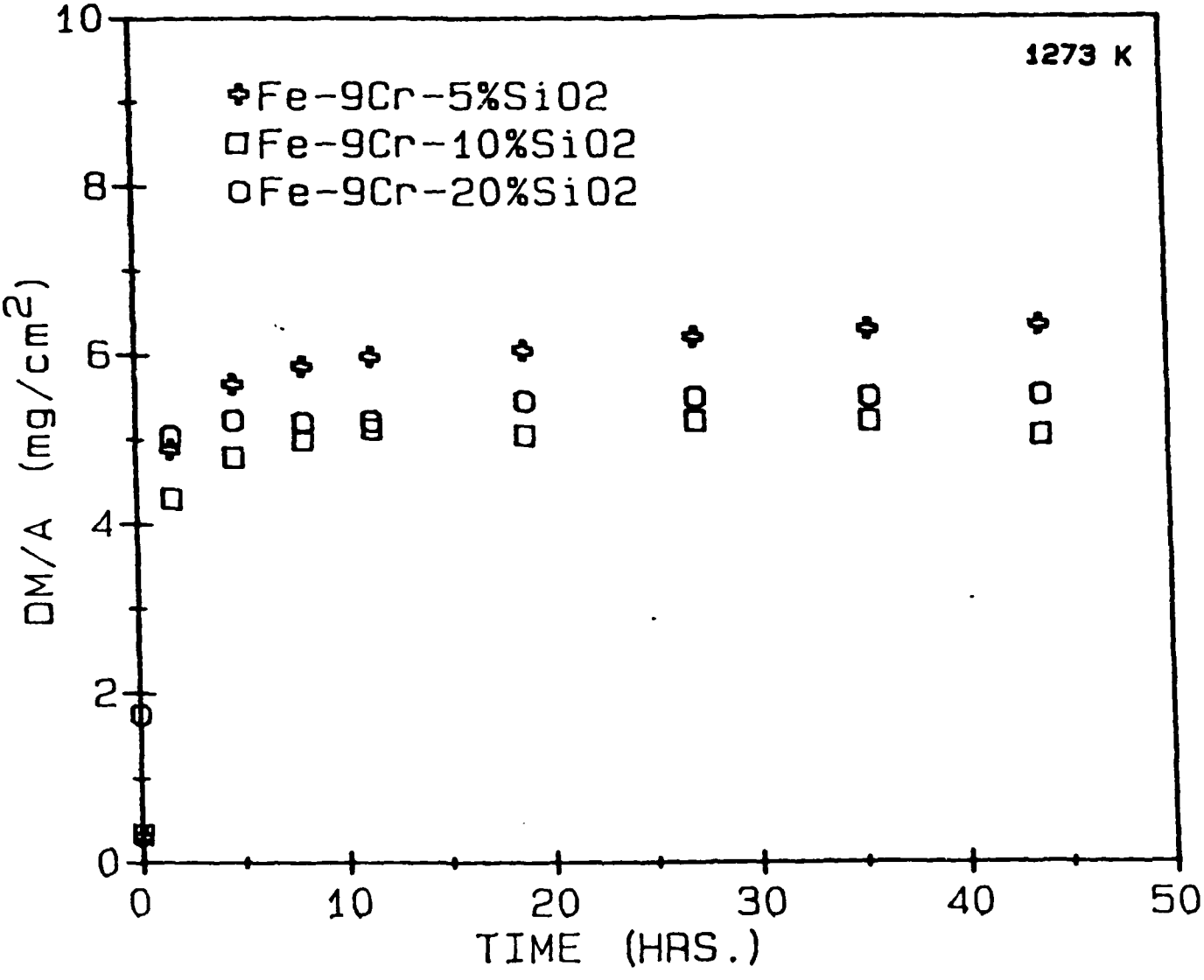

Figure 19. Isothermal oxidation curves for binary Fe-9Cr alloys containing SiO_2 particles at 1273 K.

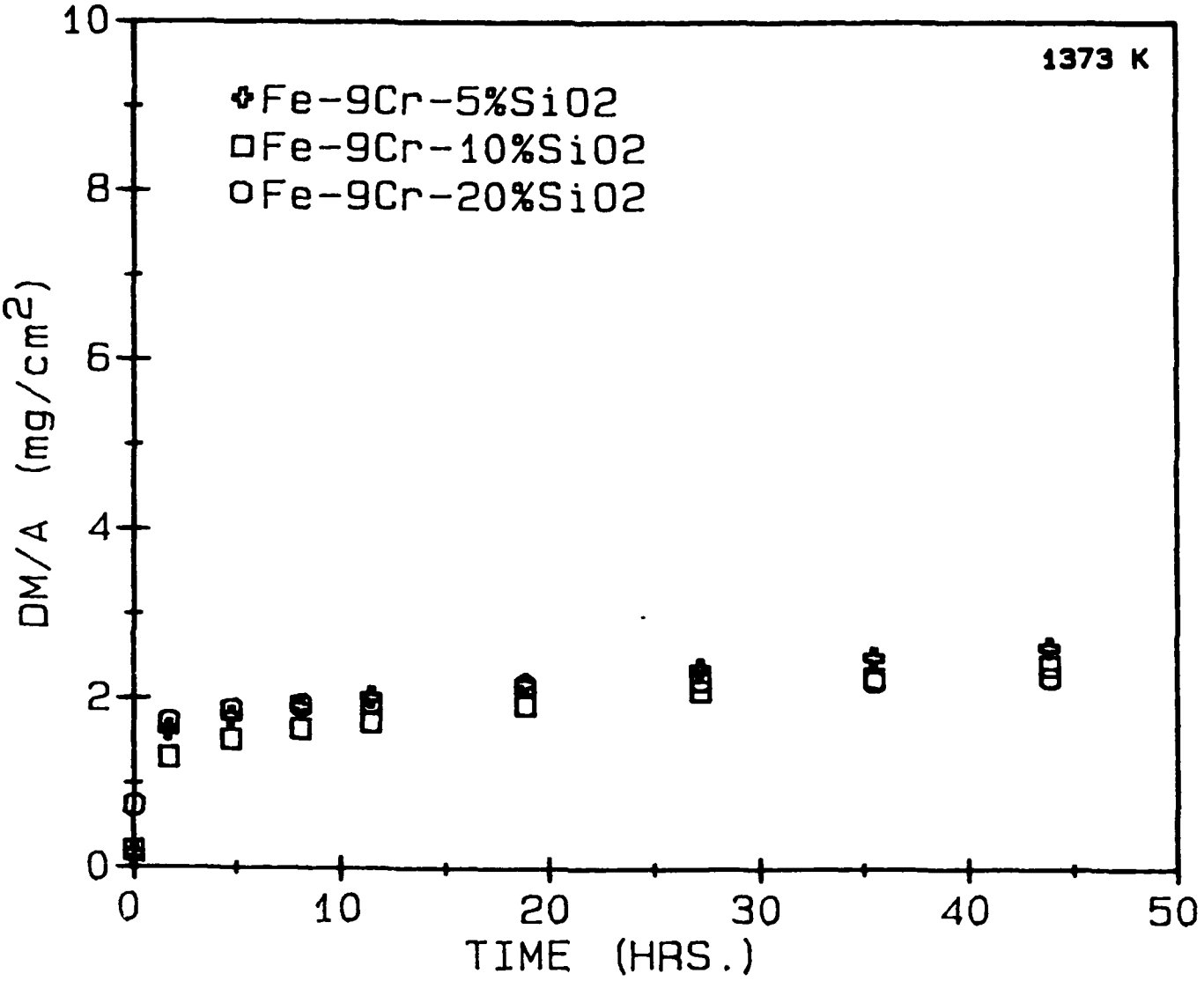

Figure 20. Isothermal oxidation curves for binary Fe-9Cr alloys containing SiO_2 particles at 1373 K.

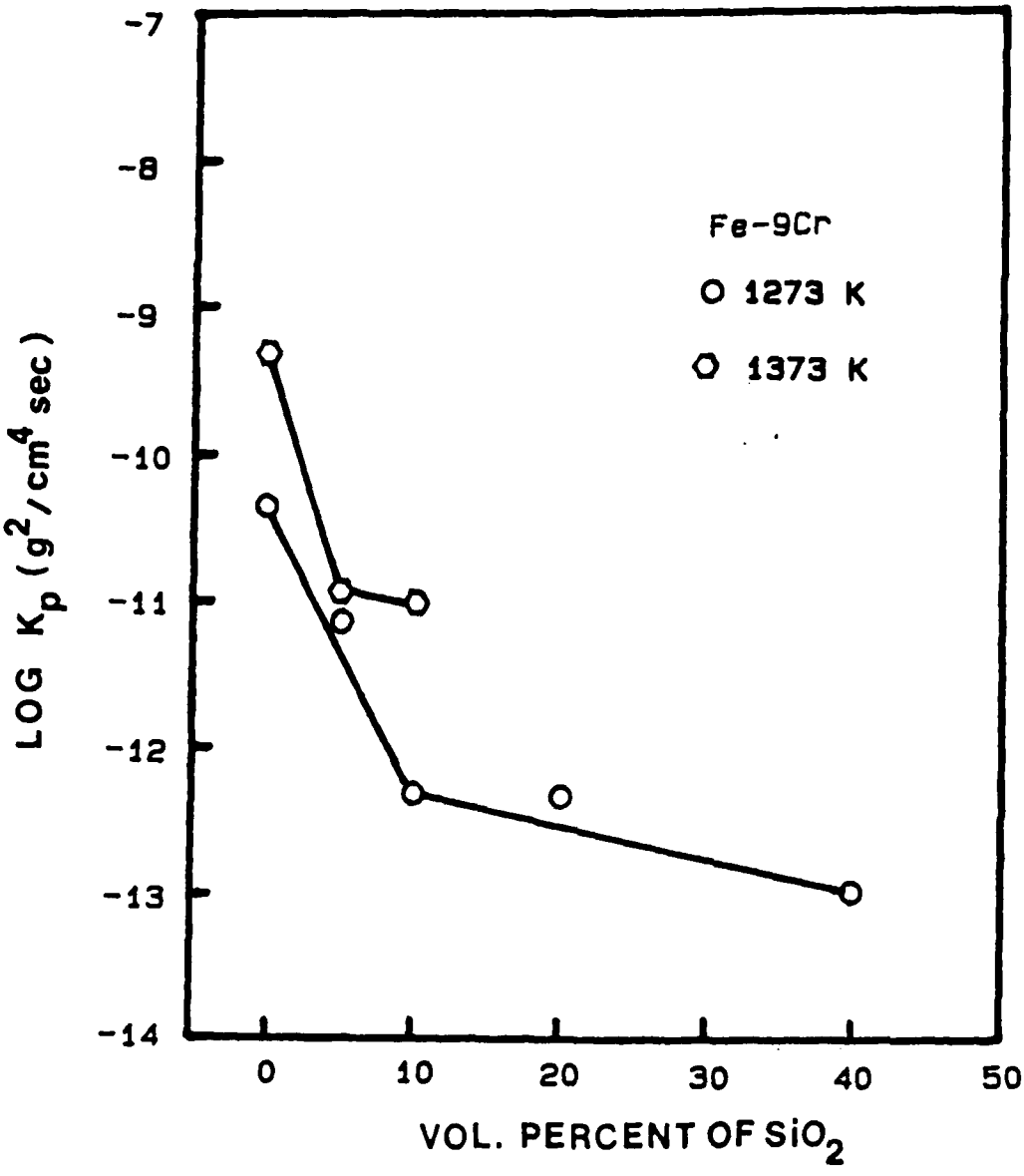

Figure 21. Parabolic oxidation rate constants of Fe-9Cr-SiO_2 alloys as a function of SiO_2 content at 1273 and 1373 K.

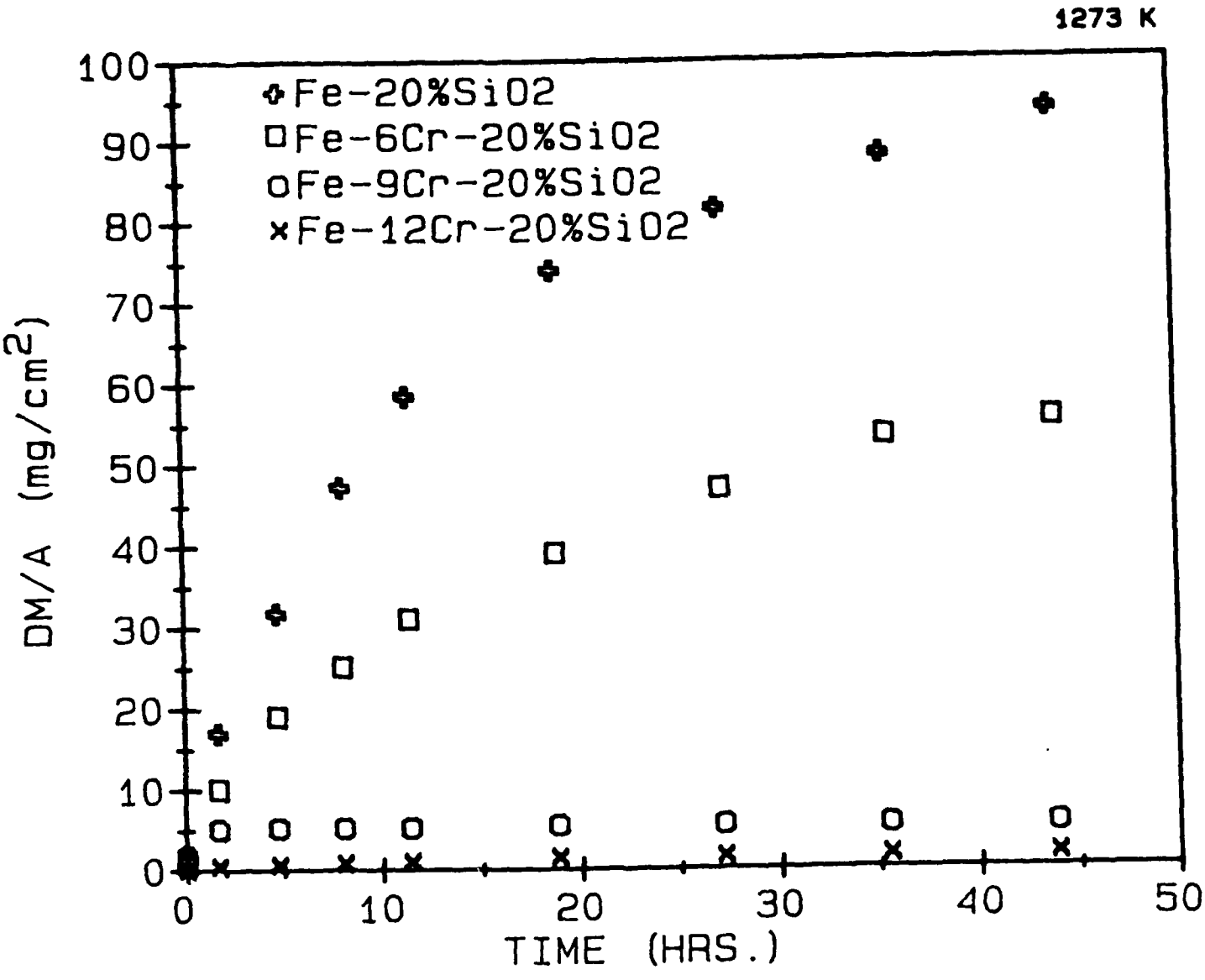

Figure 22. Isothermal oxidation curves for Fe-Cr alloys with a constant SiO_2 content (20 vol%).

END

FILMED

FEB. 1988

DTIC